1992

Dynamics of an Orbiting Scroll with Axial Compliance, Part 2 - Experimental Techniques

J. Marchese
United Technologies Research Center

DYNAMICS OF AN ORBITING SCROLL WITH AXIAL COMPLIANCE
Part 2 - Experimental Techniques

Anthony J. Marchese
(203)727-7785
Assistant Research Engineer

United Technologies Research Center
Silver Lane - M.S. 19
East Hartford, CT 06108

ABSTRACT

In scroll compressors equipped with axial compliance mechanisms, the orbiting scroll may be exhibit axial motion, particularly during transient conditions at startup and shutdown. An experimental effort was undertaken to measure the instantaneous pressures acting on, and the rigid body motion of, an axially compliant orbiting scroll. For a rigid body, the <x,y,z> coordinates of any three points are sufficient to describe rigid body motion. Accordingly, three proximity probes located approximately 120 degrees apart, were installed beneath the orbiting scroll to measure the axial position of three points on the underside of the orbiting scroll baseplate. The remaining x and y coordinates were available from geometry and instantaneous crank angle measurement. High response axial compliance pressure, high response compression chamber pressures, and proximity probe data were acquired for various operating conditions at steady state, startup and shutdown. Results indicated that the duration of orbiting scroll "wobble" at transient startup conditions was a function of compliant chamber volume, port diameter and seal configuration. A computer model was written to optimize the compliance chamber to essentially eliminate the duration of orbiting scroll wobble during compressor startup. During compressor shutdown, the orbiting scroll remained stable.

NOMENCLATURE

C_v	Constant volume specific heat of refrigerant, btu/lbm-R.
d_{sl}	Diameter of compliance chamber supply line, in.
e_{sl}	Roughness of compliance chamber supply line, in.
h_{sl}	Enthalpy of gas entering compliance chamber, btu/lbm.
l_{sl}	Length of compliance chamber supply line, in.
m	Instantaneous mass in compliance chamber, lbm.
$\dot{m}_{sl}$	Instantaneous flow rate into compliance chamber, lbm/s.
P	Instantaneous pressure in compliance chamber, psia.
P_c	Instantaneous pressure in compression chamber, psia.
T	Instantaneous temperature in compliance chamber, R.
T_c	Instantaneous temperature in compression chamber, R.
t	Time, s.
V_{bc}	Compliance chamber volume, in^3.
v	Velocity of gas entering compliance chamber, ft/s.
z	Axial displacement of orbiting scroll baseplate, in.
z_c	Total axial clearance between scroll elements, in.
ρ	Instantaneous density of gas in compliance chamber, lb/in_3.

INTRODUCTION

In order to obtain high efficiency in a scroll compressor, some means of minimizing tip leakage is necessary. One method of minimizing tip leakage is to incorporate seals into the tips of the scroll flanks [1]. A second approach is to pressurize a cavity located beneath an axially compliant orbiting scroll. This approach generates an upward force on the orbiting scroll greater than the downward force generated by gas compression [2]. A third approach entails pressurizing a cavity above an axially compliant fixed scroll creating a downward force on the fixed scroll which is in excess of the upward pressure forces created by gas compression [3].

For a scroll compressor equipped with a compliance chamber beneath an axially compliant orbiting scroll, the primary design criterion is to provide enough upward force beneath the orbiting scroll to not only overcome the downward compression force, but to counteract the orbiting scroll overturning moment as well. An optimum design would accomplish these functions with a minimum of excess upward force so as to minimize friction between the scroll elements. Upward force is generated by bleeding high pressure compression and/or discharge gas through the orbiting scroll baseplate into the compliance chamber.[4,5] If insufficient force is generated by the compliant chamber, even for a portion of the cycle, the orbiting scroll can become unstable, resulting in axial vibrations, or "wobble".

Much work has been done to ensure stability of the orbiting scroll during steady state operation. In typical compressor applications, however, a scroll compressor will spend much of its lifetime cycling on and off. To ensure maximum reliability, it is therefore prudent to design an axial compliance device which is not only stable at steady state conditions, but results in minimal instability during transient compressor startup and shutdown conditions. Accordingly, an analytical dynamic model of the orbiting scroll, applicable to steady state and transient conditions, is under development for use as a design optimization tool for axial compliance mechanisms [6]. In order to validate this model, and to gain valuable insight into the behavior of a scroll compressor during the first several seconds immediately after startup and shutdown, a laboratory prototype compressor was extensively instrumented and tested during transient and steady state operation.

EXPERIMENTAL PROCEDURE

Instrumentation

To perform the experiments described in this paper, the laboratory test compressor was instrumented with 4 high response proximity probes and 7 high response pressure transducers. For a 3-D rigid body, the coordinates of any three points are sufficient to describe rigid body motion. Accordingly, three proximity probes, located approximately 120 degrees apart, were installed beneath the orbiting scroll to measure the axial displacement of the orbiting scroll baseplate. A fourth proximity probe was installed to generate a signal which featured a sharp pulse at a known crank angle for use as a crank angle reference and speed pickup. Figure 1 shows the installation locations of the proximity probes.

One high response pressure transducer was located in the axial compliance chamber beneath the orbiting scroll (Fig. 1) to measure instantaneous pressure within the chamber. The remaining six high response pressure transducers were located in the fixed scroll to measure instantaneous suction, compression, and discharge port pressures. These pressure transducers were used to track the pressure of a fluid element as it traveled from suction to discharge during steady state or transient compressor operation [7]. Figure 2 shows the installation locations of the pressure transducers.

Data System

The data were acquired, stored, reduced, displayed, and plotted using a state-of-the-art data system at United Technologies Research Center (UTRC). This completely software driven data system features a real-time data acquisition computer and X-window terminals at 5 separate calorimeter and desuperheater test stands. The system is configured with multiple thermocouple channels, steady state channels, and high speed channels, and is shown schematically in Figure 3.

Test Procedure

The laboratory test compressor was integrated into a desuperheater test stand equipped with suction and discharge pressure transducers and thermocouples which enabled accurate determination of operating condition [8]. Figure 4 shows the compressor in test configuration. Prior to gathering the transient data, the compressor was operated to establish the proper valve settings to achieve the desired steady state operating condition. The compressor power was then turned off. As power was restored, instantaneous suction pressure, discharge pressure, compression pocket pressures, compliance chamber pressure, orbiting scroll baseplate proximity probe data, and crank angle reference data were acquired for the initial 2 seconds during the transient compressor startup.

The compressor was then allowed to run for approximately 2 hours until it was determined that temperatures measured in the motor, bearings, shell, and oil sump had reached steady state. Once the compressor temperatures reached steady state,. the input power to the compressor was terminated while the above pressure data and proximity data were acquired during the transient compressor shutdown.

TEST RESULTS

Proximity Probe Electronic Runout

From previous experience with high response proximity probes, it was understood that the raw output signal from each proximity probe would contain not only information related to axial displacement of the orbiting scroll baseplate, but electronic runout as well. Electronic runout is an error signal introduced by nonuniform electrical and mechanical properties of the area of the orbiting scroll baseplate observed by each probe. In order to accurately measure the electronic runout of each proximity probe, the drive train and orbiting scroll were assembled into the center portion of the semi-hermetic test shell as shown in Figure 5.

A computer program was written to acquire the proximity probe data at 10 degree intervals of crank angle while the shaft was rotated. The computer program fit a cubic spline through the runout data so that it could be digitally subtracted from the raw proximity probe signals acquired throughout the subsequent tests described below. It was possible to perform the digital signal processing on a real-time basis using the laboratory data system. Figure 6 shows one cycle of raw proximity probe data generated during operation of the laboratory compressor plotted with the electronic runout for probe 1. This figure clearly shows that a substantial portion of the raw signal can, indeed, be attributed purely to electronic runout rather than actual axial displacement of the orbiting scroll.

Compressor Startup

Figure 7 shows the suction, compression, and discharge pressures in the scroll compressor for approximately the first 60 shaft revolutions. These results showed that the laboratory scroll compressor approached full speed after only 3 to 4 shaft revolutions. The radial compliance mechanism engages quickly, resulting in compression pocket pressures which quickly approached their steady state values. As a consequence, the axial pressure force and overturning moment exerted on the orbiting scroll also quickly approached their steady state value. This required an axial compliance device which energized quickly to ensure negligible orbiting scroll wobble at startup. In order to optimize the axial compliance pressure chamber for transient startup conditions, a computer model similar to the steady state model described in Ref. [4] was developed for transient conditions.

The transient model used the transient pressures (Fig. 7) as input and assumed Fanno Flow (constant area, adiabatic, with friction) in the compliance chamber supply line. The conservation of mass, conservation of energy, and the refrigerant gas equation of state were used to calculate transient pressure in the compliance chamber according to the following equations:

$$\dot{m}_{sl} = \dot{m}(Pc_i, Tc_i, P_{i-1}, T_{i-1}, d_{sl}, l_{sl}, e_{sl}) \tag{1}$$

$$m_i = m_{i-1} + \dot{m}_{sl}\ \Delta t \tag{2}$$

$$\rho_i = m_i / V_{bc} \tag{3}$$

$$T_i = T_{i-1}(1 - \Delta t\ \dot{m}_{sl}/m_i) + \frac{\Delta t\ \dot{m}_{sl}}{\overline{m}_i\ \overline{C}v_{i-1}} (h_{sl,i} + V_i^2/2) \tag{4}$$

$$P_i = P(T_i\ ,\ \rho_i). \tag{5}$$

This finite-difference analysis indicated that the transient compliance chamber pressure rise time is a function of chamber volume, supply port diameter, supply line length, and supply port location. Figure 8 is a plot of predicted and measured compliance chamber pressure for two different supply port diameters and chamber volumes. This figure shows the trade-off between transient rise time and steady state pressure pulsation. It is apparent that the larger values of $d/V^{1/3}$ (corresponding to larger line size and/or smaller compliance chamber volume) result in faster initial pressure rise and larger steady state pressure pulsations.

Figure 9 shows plots of the three proximity probe signals during transient startup conditions for the two different geometries. The normalized axial displacement z/z_c shown in these figures is the displacement of the orbiting scroll baseplate from the bottom of the fixed scroll surface divided by the total axial clearance between the fixed and orbiting scrolls. This figure indicates that the duration of orbiting scroll instability can be minimized by minimizing the compliance chamber pressure rise time.

Compressor Shutdown

In order to exaggerate the duration of reverse rotation encountered during compressor shutdown, the internal check valve was removed and replaced with a check valve in the discharge line external to the compressor. Figure 10 is a plot of compression chamber pressures during compressor shutdown for the laboratory scroll compressor in this configuration. This figure shows that when the input power was terminated, the high pressure on the discharge side of the compressor relieved through the scroll elements, causing the compressor to run in reverse. At this condition, flow reversal occurred at about 0.4 seconds causing the laboratory scroll compressor to run in reverse for about 30 shaft revolutions.

During this reverse rotation, the orbiting scroll exhibited little axial instability. This was because the compliance chamber remained sufficiently pressurized to generate upward axial forces great enough to overcome the decreasing downward axial force and overturning moment. Figure 11 shows the compliance chamber pressure and the proximity probe data during reverse rotation ($t > 0.4$ seconds).

Since the orbiting scroll exhibits little axial instability during reverse rotation, compressor shutdown does not appear to adversely effect compressor reliability. Reverse rotation does, however, result in an undesirable noise whose duration is directly related to the volume of the high pressure gas on the discharge side. Thus, one way to minimize the duration of reverse rotation is to place the check valve as close as possible to the discharge port of the scroll elements. Accordingly, the internal check valve was re-installed into the laboratory compressor directly downstream from the fixed scroll discharge port. Figure 12 is a plot of compression chamber pressures during shutdown with the internal check valve in place. This figure shows that in this configuration the laboratory scroll compressor exhibited zero reverse rotations and consequently no orbiting scroll wobble.

CONCLUSIONS

Proper design of the axial compliance mechanism can effectively minimize or even eliminate axial movement of the orbiting scroll during transient startup. Such an axial compliance mechanism will also prevent orbiting scroll axial motion during the reverse rotation encountered during compressor shutdown in scroll compressors installed with external discharge line check valves. In scroll compressors equipped with an internal check valve, little or no reverse rotation occurs at shutdown, resulting in no orbiting scroll axial motion.

Transient pressures acting on the orbiting scroll and resulting orbiting scroll axial motion can be accurately determined using appropriate instrumentation together with a state-of-the-art data system. The orbiting scroll axial vibration characteristics derived in this manner have provided a fundamental understanding of the orbiting scroll dymamics during steady state and transient operation. These experimental results will be used for validating the analytical model described in reference [6]. The experimental techniques described herein, together with continued development of the dynamic model provide a valuable tool for the scroll compressor designer.

ACKNOWLEDGMENTS

The author wishes to acknowledge the assistance of UTRC researchers Jack Shu, Ray DeBlois, Gerry Cloutier and Larry Hardin; and Tom Barito at Carrier.

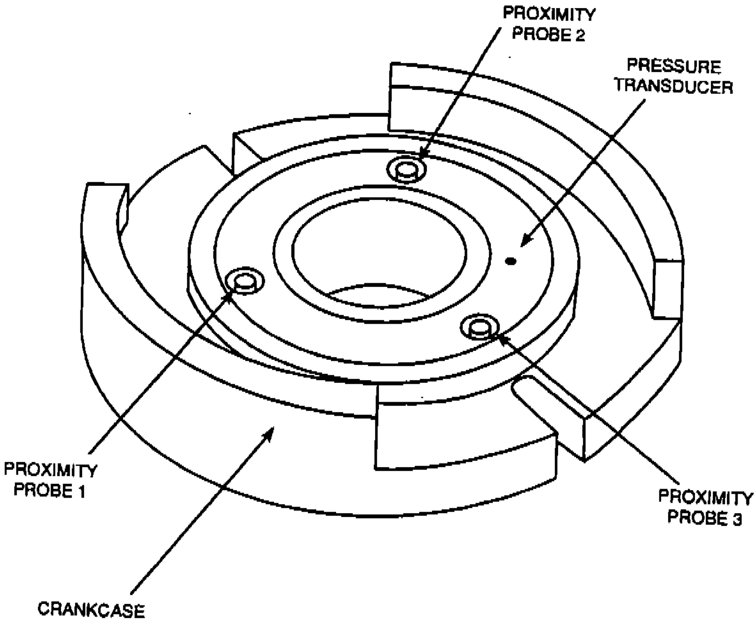

Figure 1. Proximity Probe Locations

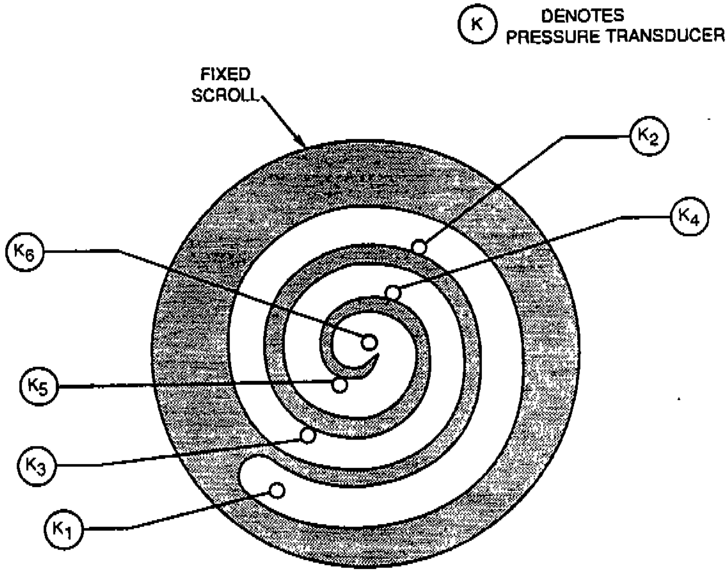

Figure 2. Compression Pocket Pressures

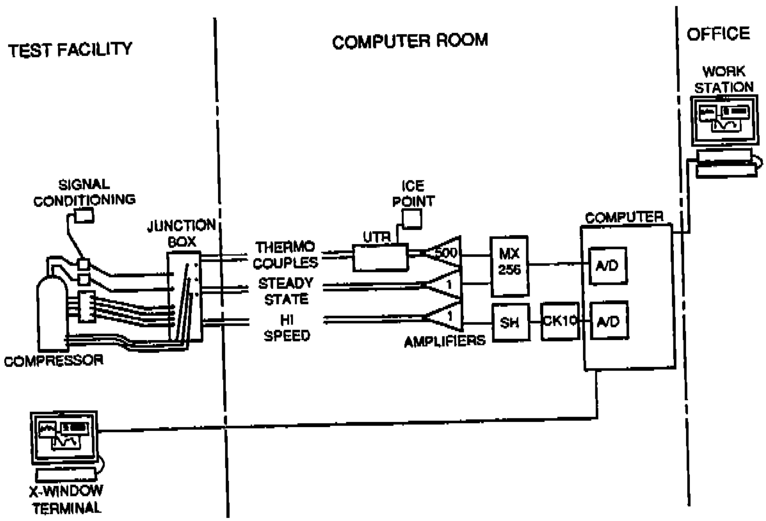

Figure 3. Data System

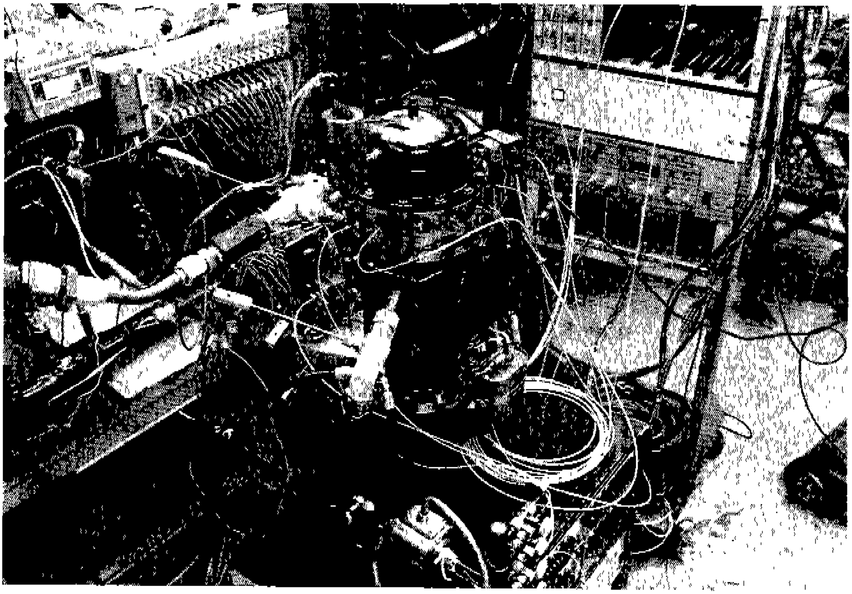

Figure 4. Laboratory Compressor in Test Configuration

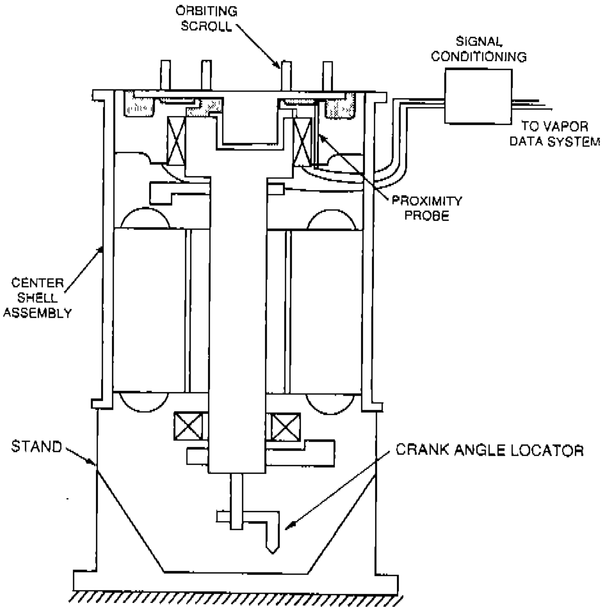

Figure 5. Determination of Proximity Probe Electronic Runout

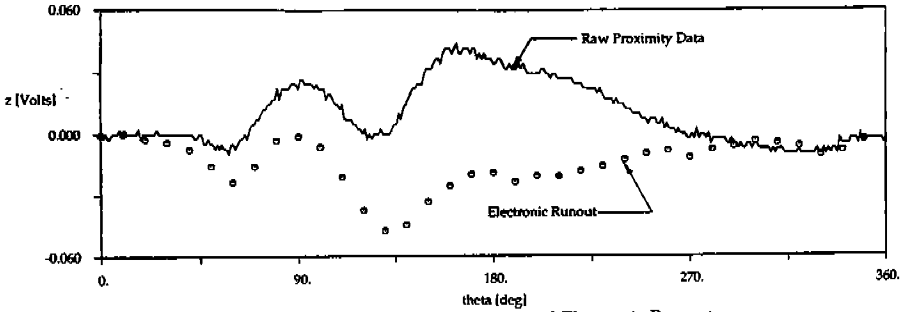

Figure 6. Raw Proximity Data and Electronic Runout

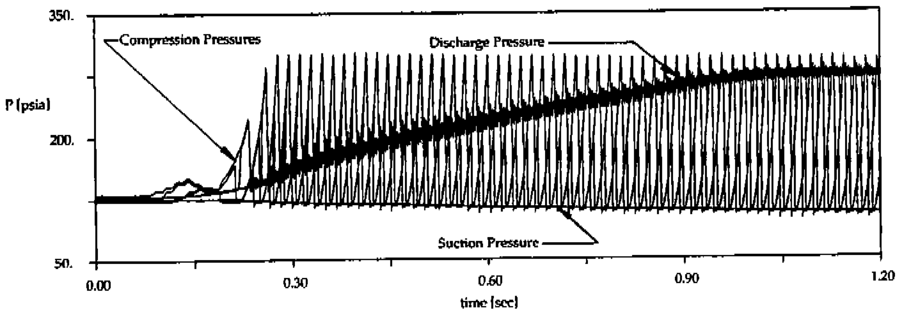

Figure 7. Compression Pocket Pressures at Startup

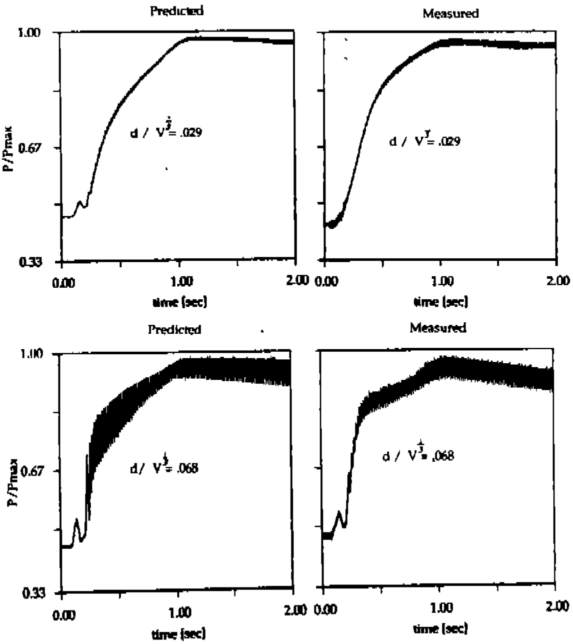

Figure 8. Compliance Chamber Pressure

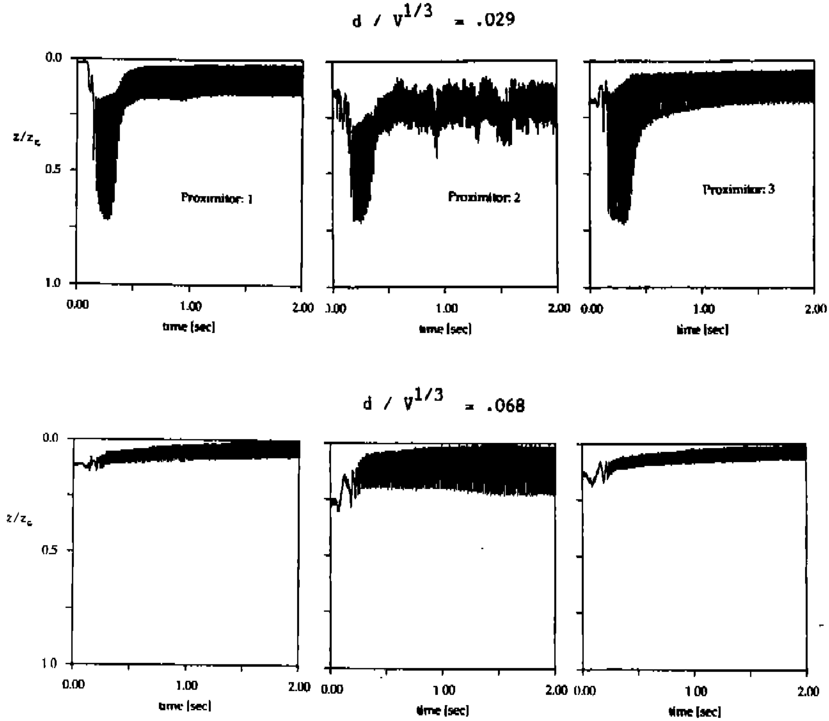

Figure 9. Orbiting Scroll Axial Displacement at Startup

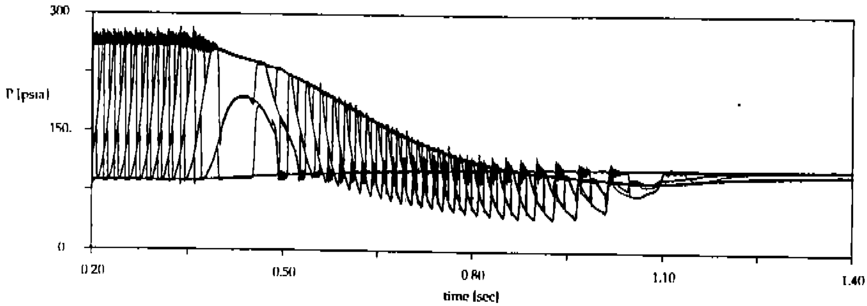

Figure 10. Compression Pocket Pressures at Shutdown

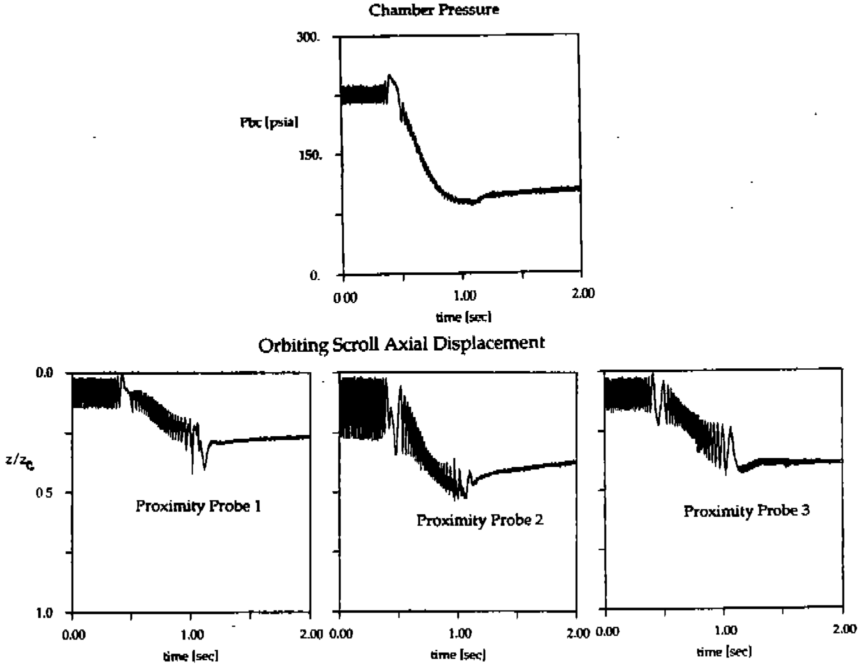

Figure 11. Compliance Chamber Pressure and Orbiting Scroll Axial Displacement at Shutdown

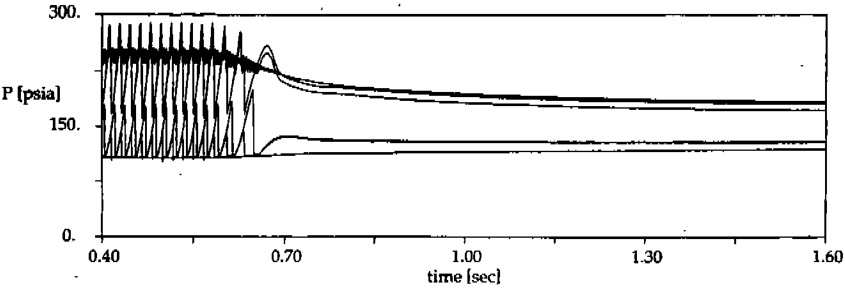

Figure 12. Compression Pocket Pressures at Shutdown with Internal Check Valve

REFERENCES

1) Inaba, Tsutomu, et al., "A Scroll Compressor with Sealing Means and Low Pressure Side Shell", Proceedings of the 1986 International Compressor Engineering Conference at Purdue, Vol. 3, pp. 887-900.

2) Tojo, Kenja, et al., "Computer model of a Scroll Compressor with Self Adjusting Back-Pressure Mechanism", Proceedings of the 1986 International Compressor Engineering Conference at Purdue, Vol 3, pp. 872-886.

3) Bush, J. W., Elson, J. P., "Scroll Compressor Design Criteria for Residential Air Conditioning and Heat Pump Applications", Proceedings of the 1988 International Compressor Engineering Conference at Purdue, Vol. 1, pp. 83-97.

4) Nieter, J. J., and Barito, Tom, "Dynamics of Compliance Mechanisms for Scroll Compressors, Part I: Axial Compliance", Proceedings of the 1990 International Compressor Engineering Conference at Purdue, Vol. 1, pp. 308-316.

5) Nieter, J. J., Marchese, A. J., and DeBlois, R. L., "Dynamic Axial Compliance to Reduce Thrust Surface Friction in a Scroll Compressor", Proceedings of the 1992 International Compressor Engineering Conference at Purdue.

6) Shu, H. T., and Peracchio, A. A., "Dynamics of an Orbiting Scroll with Axial Compliance, Part 1: Simulation of Orbiter Motion", Proceedings of the 1992 International Compressor Engineering Conference at Purdue.

7) DeBlois, R. L., and Stoeffler, R. C., "Instrumentation and Data Analysis Techniques for Scroll Compressors", Proceedings of the 1988 International Compressor Engineering Conference at Purdue, Vol. 1, pp. 182-188.

8) McGovern, J. A., "Analysis of a Refrigerant Compressor Load Stand Incorporating Hot Gas Bypass and a Single Full Condensation Heat Exchanger", Proceedings of the 1984 International Compressor Engineering Conference at Purdue, Vol 1., pp. 468-477.